J|A|C|S
COMMUNICATIONS

Published on Web 12/16/2003

Measurement of Five Dipolar Couplings from a Single 3D NMR Multiplet Applied to the Study of RNA Dynamics

Erin O'Neil-Cabello,[†,‡] David L. Bryce,[†] Edward P. Nikonowicz,[‡] and Ad Bax*,[†]

Laboratory of Chemical Physics, NIDDK, National Institutes of Health, Bethesda, Maryland 20892-0520, and Department of Biochemistry and Cell Biology, Rice University, P.O. Box 1892, Houston, Texas 77251

Received September 3, 2003; E-mail: bax@nih.gov

Access to orientational information through the measurement of short-range dipolar couplings in weakly oriented molecules has created new opportunities for the structure determination of proteins[1−3] and nucleic acids[4−7] by NMR. The ability to determine a local order matrix, and thereby define dynamics along a protein backbone[8] or in different regions of multisubunit nucleic acids,[9] offers the possibility of gaining unique insights not only into the time-averaged structure, but also into the degree of internal dynamics, averaged over the entire time regime from milli- to femtoseconds.[10]

A prerequisite for determining local order in a single alignment medium is that dipolar couplings are available for an element of known local structure, containing at least five different internuclear vectors. Here, we demonstrate a simple and accurate experiment for measurement of five such couplings from a single E.COSY[11] cross-peak pattern for the ribose sugars in an RNA oligomer. The couplings are extracted from the H1′−C1′−C2′−H2′ ribose spin system. Analogous to the protein triple resonance naming convention, we refer to this "out-and-back" experiment as H1C1C2. The experiment (Figure 1) transfers magnetization from H1′ via H1′−C1′ multiple quantum coherence to C2′, which then evolves as single quantum coherence during the constant-time (CT) evolution period t_1 ($1/J_{C1'C2'} = 25$ ms) and is transferred back to C1′ (CT t_2 evolution) and H1′ (detection, t_3). No ^{1}H decoupling is applied so that the ^{13}C−{^{1}H} doublet components in the F_1 and F_2 frequency dimensions are separated by $^1J_{C2'H2'} + {}^1D_{C2'H2'}$ and $^1J_{C1'H1'} + {}^1D_{C1'H1'}$, respectively. Because no ^{1}H pulse is applied between the t_1 and t_2 evolution periods, protons retain their spin state and the two C1′−{H1′} doublets are displaced relative to one another by $^2J_{C1'H2'} + {}^2D_{C1'H2'}$ (Figure 2A). Similarly, the two C2′−{H2′} doublets are displaced by $^2J_{C2'H1'} + {}^2D_{C2'H1'}$. A fifth coupling, $^3J_{H1'H2'} + {}^3D_{H1'H2'}$, is available from the F_3 displacement between the downfield and upfield C2′−{H2′} doublets (Figure 2B). This displacement is caused by the final Rance−Kay magnetization transfer from C1′ to H1′, which does not change the H2′ spin state due to the C1′-selective nature of the ^{13}C 180° pulses, analogous to an invariant H^α spin state in HNCA-type E.COSY measurements of $^3J_{HNH\alpha}$.[12] Because of relaxation during the Rance−Kay transfer, not all of the H2′ spins return to their original spin state, resulting in a ca. 20% reduction in the ^{1}H−^{1}H E.COSY displacement for the RNA oligomer studied here.[13]

Because of the high efficiency of each magnetization transfer step, the sensitivity of the H1C1C2 experiment is good, despite the presence of two CT periods, of durations $1/J_{C1'C2'}$ for t_1 and $1/(2J_{C1'C2'})$ or $3/(2J_{C1'C2'})$ for t_2. Experiments were carried out at 800 MHz on a sample containing 1.9 mM uniformly ^{13}C enriched RNA oligomer, derived from helix-35 of *E. coli* 23S ribosomal RNA (Figure 2C). Couplings were measured in the isotropic state

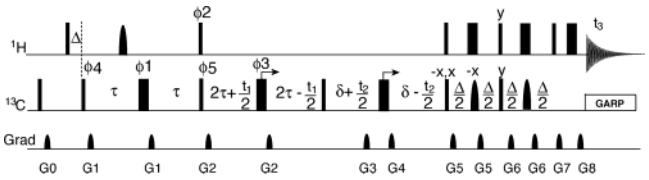

Figure 1. Pulse sequence of the H1C1C2 experiment. Narrow bars and wide bars represent 90° and 180° pulses, respectively. Unless otherwise indicated, all pulses have phase *x*. Shaped pulses are of the 180° reBURP type[19] and have durations of 2.7 (centered at H1′) and 1.0 ms (C1′) at 800 MHz ^{1}H frequency. Delay durations: $\Delta = 1/2J_{C1'H1'}$, $\tau = 1/4J_{C1'C2'}$. For the C1′ constant-time evolution period, $\delta = 1/4J_{C1'C2'}$ for optimal signal-to-noise; $\delta = 3/4J_{C1'C2'}$ for optimal F_2 resolution. Phase cycling: $\phi_1 = 4(-y),4(x)$; $\phi_2 = 2(y),2(-y)$; $\phi_3 = x,y$; $\phi = y$; $\phi = x$; receiver $= x,-x,-x,x,-x,x,x,-x$. Quadrature detection was obtained in the ^{13}C dimension by simultaneously incrementing ϕ_1, ϕ_4, and ϕ_5 in the regular States-TPPI manner. Pulsed field gradients are sine-bell shaped with durations of $G_{0,1,2,3,4,5,6,7,8} = 0.25$, 0.4, 0.4, 1.0, 1.0, 0.25, 0.25, 0.203, 0.3 ms, peak amplitudes of $G_{0,1,2} = 40$ G/cm; $G_{3,5,7} = 50$ G/cm; $G_{4,8} = -50$ G/cm; $G_6 = 30$ G/cm, and directions of $G_{0,1,2,5,6} = z,z,y,y,(xy)$, $G_{3,4,7,8} = (xyz)$.

and in the presence of 22 mg/mL of liquid crystalline Pf1[14] (Supporting Information). In the absence of overlap, two independent measures are available for each splitting (Figure 2), and their pairwise reproducibility provides an estimate of the random error: ≤0.5 Hz for $^1J_{C2'H2'} + {}^1D_{C2'H2'}$ and $^2J_{C2'H1'} + {}^2D_{C2'H1'}$ in the aligned medium, and somewhat better for the isotropic values, due to the higher signal-to-noise ratio. Because of the higher F_3 resolution, reproducibility is best for $^3J_{H1'H2'} + {}^3D_{H1'H2'}$, ≤0.3 Hz. Thus, the measurement error for the $^2D_{C2'H1'}$, $^2D_{C1'H2'}$, and $^3D_{H1'H2'}$ couplings is small relative to the observed range of these couplings (Supporting Information).

As expected,[15,16] the isotropic values for $^1J_{C1'H1'}$, $^2J_{C1'H2'}$, and $^3J_{H1'H2'}$ clearly correlate with the ribose ring pucker: In the A-form stem region, where ribose ring puckers are C3′-endo, we find $^1J_{C1'H1'} = 175.5 \pm 0.5$ Hz for purines, 179.4 ± 0.5 Hz for pyrimidines; $^1J_{C2'H2'} = 157.5 \pm 0.5$ Hz for purines, 159.1 ± 0.5 Hz for pyrimidines; $^2J_{C1'H2'} = 2.6 \pm 0.2$ Hz for purines, 2.0 ± 0.2 Hz for pyrimidines; $^2J_{C2'H1'} = -1.7 \pm 0.5$ Hz for purines, -2.5 ± 0.5 Hz for pyrimidines; $^3J_{H1'H2'} \leq 1.5$ Hz for both purines and pyrimidines. Values considerably outside of these ranges are found for many of the loop nucleotides (Supporting Information).

With the exception of ψ746, for which C1′ resonates outside the region selected by the shaped ^{13}C pulses, and the terminal G737 which is not ^{13}C-enriched, a complete set of five dipolar couplings was obtained for each nucleotide. An SVD fit of the stem region (G738-U744/A753-C759) dipolar couplings to a model A-form RNA helix (PDB entry 1QCU) yields values for the magnitude and rhombicity of the alignment tensor: $D_a^{CH} = -20.8$ Hz, $R = 0.31$ (Supporting Information). A systematic grid search as a function of D_a^{CH} and R of the alignment tensor,[17] allowing its orientation to vary, is then applied to individual riboses that are constrained to C3′-endo on the basis of their J couplings. Such a

[†] National Institutes of Health.
[‡] Rice University.

10.1021/ja038314k CCC: $27.50

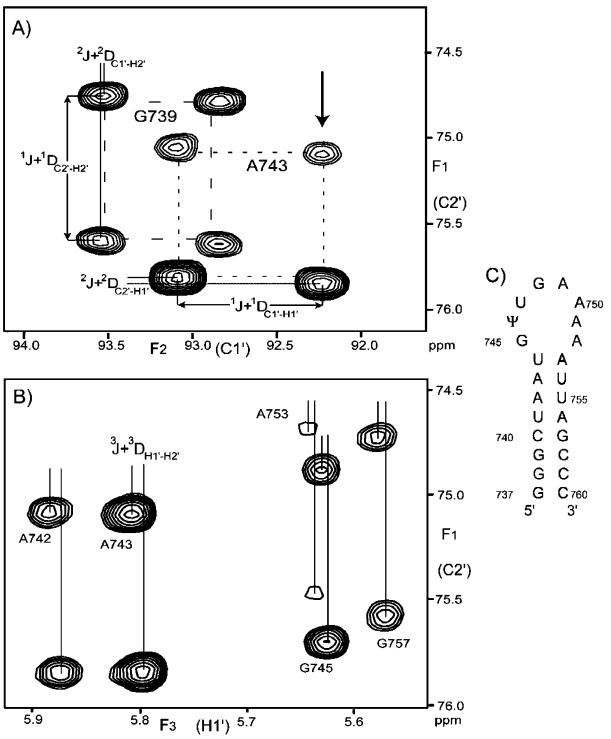

Figure 2. Cross sections taken through the 800 MHz 3D H1C1C2 NMR spectrum of the RNA shown in (C), recorded with a short t_2 (C1′) evolution period of 11.7 ms, in the presence of 22 mg/mL of Pf1 ($t_{1,\max}$ = 24.3 ms, $t_{3,\max}$ = 68.2 ms; total measuring time 18 h). (A) Small region of a ^{13}C−^{13}C plane, taken at F_3 (^{1}H) = 5.79 ppm, showing ^{1}H-coupled C1′−C2′ correlations for G739 (multiplet components connected by long dashes), and for A743 (short dashes). Separation between multiplet components corresponds to the marked couplings of interest. In the absence of overlap, two independent measurements of each coupling are available per residue; only one set of these is marked. (B) Small region of a C2′−H1′ (F_1,F_3) cross section, taken at F_2 (C1′) = 92.26 ppm (at the position marked by an arrow in (A)), displaying correlations for A743 and four other nucleotides. F_3 displacement between the doublet components corresponds to the H1′−H2′ coupling.

grid search reveals all D_a^{CH} and R combinations that fit the data within experimental error.[17] Results indicate that D_a^{CH} and R are uniform throughout the stem (Supporting Information). However, when the same analysis is applied to the terminal nucleotide, C760 (also in a C3′-endo conformation on the basis of its J couplings), a 15% reduction of D_a^{CH} is found (Figure 3). This smaller alignment magnitude is attributed to increased motion of the terminal nucleotide relative to the stem. Interestingly, most of the grid search solutions that fit the data within experimental error (contoured region in Figure 3) indicate increased rhombicity for C760 relative to the stem. Note that, in general, dynamics of a rigid element such as a C3′-endo ribose relative to the overall structure will scale its alignment tensor principal components differentially, that is, alter its rhombicity.[10]

Most loop riboses have $^3J_{H1'H2'}$ and dipolar couplings that are incompatible with a C3′-endo conformation. For example, for A749, only a C4′-exo pucker (or a dynamic average of different puckers) satisfies the dipolar couplings (Supporting Information). A grid search analysis, using such a C4′-exo reference structure, indicates a reduction in D_a^{CH} by ca. 50% for A749 relative to the stem (Supporting Information).

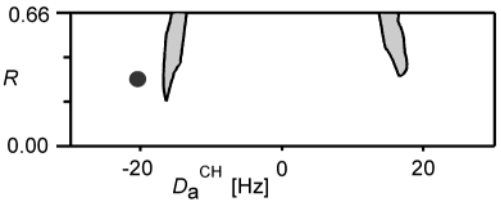

Figure 3. Evidence for reduced effective alignment of the terminal C760 in helix-35ψ^{746} RNA. The contour plot outlines the region where D_a^{CH} and R values for a C3′-endo ribose are compatible with all C760 dipolar couplings (solid contour at $\chi^2 \le \epsilon^2 = 4$ Hz^2, that is, corresponding to a $\epsilon = 2$ Hz error in the normalized dipolar couplings). Besides $^1D_{C1'H1'}$, $^1D_{C2'H2'}$, $^2D_{C2'H1'}$, $^2D_{C1'H2'}$, and $^3D_{H1'H2'}$, experimental values for $^1D_{C1'C2'}$, $^1D_{C3'H3'}$, and $^1D_{C4'H4'}$ were also included in generating the contour. The solid dot marks the D_a^{CH} and R values from an SVD fit of couplings from the helical stem to an A-form RNA helix (PDB entry 1QCU) and corresponds to $\chi^2/N = 12.8$ Hz^2 for the C760 couplings.

Simultaneous measurement of five dipolar couplings from a single cross-peak pattern is easily adapted to numerous other spin systems, including C$^\alpha$ sites in proteins, and H6−C6−C5 fragments in pyrimidine bases. For this latter application, where all vectors are in a single plane, only three dipolar couplings carry independent information, but the availability of five measured values can be used to check internal consistency of the experimental data.[18]

Acknowledgment. This work was supported by NIH Training Grant 08280 (to E.O.-C.), the R. A. Welch Foundation (C1277) and NSF (MCB-0078501) (both to E.P.N.), and NSERC (to D.L.B.).

Supporting Information Available: Two tables with ribose J and dipolar couplings for helix-35ψ^{746}, plots of SVD versus measured couplings, systematic pseudorotation angle search results, grid search (D_a^{CH}, R) results for stem riboses, and grid search for A749 (PDF). This material is available free of charge via the Internet at http://pubs.acs.org.

References

(1) Tolman, J. R.; Flanagan, J. M.; Kennedy, M. A.; Prestegard, J. H. *Proc. Natl. Acad. Sci. U.S.A.* **1995**, *92*, 9279−9283.
(2) Tjandra, N.; Bax, A. *Science* **1997**, *278*, 1111−1114.
(3) Tugarinov, V.; Kay, L. E. *J. Mol. Biol.* **2003**, *327*, 1121−1133.
(4) Bayer, P.; Varani, L.; Varani, G. *J. Biomol. NMR* **1999**, *14*, 149−155.
(5) Lynch, S. R.; Puglisi, J. D. *J. Am. Chem. Soc.* **2000**, *122*, 7853−7854.
(6) Vermeulen, A.; Zhou, H. J.; Pardi, A. *J. Am. Chem. Soc.* **2000**, *122*, 9638−9647.
(7) Al-Hashimi, H. M.; Gorin, A.; Majumdar, A.; Gosser, Y.; Patel, D. J. *J. Mol. Biol.* **2002**, *318*, 637−649.
(8) Tolman, J. R. *J. Am. Chem. Soc.* **2002**, *124*, 12020−12030.
(9) Al-Hashimi, H. M.; Pitt, S. W.; Majumdar, A.; Xu, W. J.; Patel, D. J. *J. Mol. Biol.* **2003**, *329*, 867−873.
(10) Meiler, J.; Prompers, J. J.; Peti, W.; Griesinger, C.; Bruschweiler, R. *J. Am. Chem. Soc.* **2001**, *123*, 6098−6107.
(11) Griesinger, C.; Sørensen, O. W.; Ernst, R. R. *J. Chem. Phys.* **1986**, *85*, 6837−6852.
(12) Madsen, J. C.; Sorensen, O. W.; Sorensen, P.; Poulsen, F. M. *J. Biomol. NMR* **1993**, *3*, 239−244.
(13) Gorlach, M.; Wittekind, M.; Farmer, B. T.; Kay, L. E.; Mueller, L. *J. Magn. Reson., Ser. B* **1993**, *101*, 194−197.
(14) Hansen, M. R.; Mueller, L.; Pardi, A. *Nat. Struct. Biol.* **1998**, *5*, 1065−1074.
(15) Podlasek, C. A.; Stripe, W. A.; Carmichael, I.; Shang, M. Y.; Basu, B.; Serianni, A. S. *J. Am. Chem. Soc.* **1996**, *118*, 1413−1425.
(16) Ippel, J. H.; Wijmenga, S. S.; deJong, R.; Heus, H. A.; Hilbers, C. W.; deVroom, E.; vanderMarel, G. A.; vanBoom, J. H. *Magn. Reson. Chem.* **1996**, *34*, S156−S176.
(17) Bryce, D. L.; Bax, A. *J. Biomol. NMR*, in press.
(18) Zidek, L.; Padrta, P.; Chmelik, J.; Sklenar, V. *J. Magn. Reson.* **2003**, *162*, 385−395.
(19) Geen, H.; Freeman, R. *J. Magn. Reson.* **1991**, *93*, 93−141.

JA038314K